

Bound state population and dissociation dynamics of a Morse oscillator with oscillating well-depth and driven by intense radiation: Perturbative and numerical studies

PRANAB SARKAR and S P BHATTACHARYYA

Department of Physical Chemistry, Indian Association for the Cultivation of Science, Jadavpur, Calcutta 700032, India

MS received 12 September 1994; revised 28 February 1995

Abstract. Bound state population dynamics in a diatom modelled by an appropriate Morse oscillator with a time-dependent well-depth is investigated perturbatively both in the absence and presence of high intensity radiation. For sinusoidally oscillating well-depth, the population of the m th bound vibrational level, $P_{mm}(t)$, is predicted to be a parabolic function of the amplitude of the oscillation of the well-depth (ΔD_0) at a fixed laser intensity. For a fixed value of ΔD_0 , $P_{mm}(t)$ is also predicted to be quadratic function of the field intensity (ϵ_0). Accurate numerical calculations using a time-dependent Fourier grid Hamiltonian (TDFGH) method proposed earlier corroborate the predictions of perturbation theory. As to the dissociation dynamics, the numerical results indicate that the intensity threshold is slightly lowered if the well-depth oscillates. Possibility of the existence of pulse-shape effect on the dissociation dynamics has also been investigated.

Keywords. Morse oscillator; time-dependent well-depth; photo dissociation.

PACS No. 33-80

1. Introduction

The quantum dynamics of a periodically forced Morse oscillator has attracted serious attention in view of its usefulness as a model for gaining insight into the response of molecular vibrations when interacting with intense radiation or laser fields [1–8]. Recent numerical studies on the dissociation dynamics of a hydrogen fluoride molecule by monochromatic sub-picosecond pulses have shown that the dissociation probability (P_d) is less than 10^{-5} when the laser intensity is below 10^{14} w/cm². Chelkowski *et al* [4–5] showed that the obtained rates of dissociation are sensitive to the shape of the excitation pulse and an appropriately chirped pulse can achieve very selective vibrational excitation with high efficiency. Brown and Wyatt [9] analyzed the bottlenecking problem in the multiphoton dissociation of a diatom modelled by a Morse oscillator under laser irradiation of high intensities. Recently, Gangopadhyay and Ray [10] proposed a theory of multiphoton excitation and dissociation of a Morse oscillator in the presence of dissipation and explored how the interplay of excitation and dissipation with the non-linearity could lead to observable effects. Adhikari *et al* [11–12] observed numerically, that the multiphoton dissociation process is characterized by the existence of a typical threshold intensity and an induction period in much the same way as the multiphoton ionization of atoms in strong laser fields [13–15]. Many more studies on different aspects of the multiphoton dissociation of molecules are also available in the current literature [16–19].

In all these studies, the Morse oscillator is characterized by a fixed time invariant well-depth which is an acceptable picture for an isolated oscillator. However, we can

imagine situations where the oscillator cannot be treated in isolation as it interacts with the surrounding media while undergoing dissociation. To be more concrete, let us think of a diatom $A-B$ undergoing multiphoton dissociation in a solvent with which it weakly interacts. We can imagine that the interaction causes temporal fluctuation of the well-depth of the Morse oscillator about the mean or the unperturbed well-depth D_0^{AB} . How does the oscillating well-depth modify the dynamics of dissociation of the diatom under strong laser irradiation? Does it alter the bound state population dynamics or affect the intensity or time thresholds observed for isolated diatoms or for Morse oscillator with constant well-depths? We propose to probe some of these questions numerically by directly solving the time-dependent Schrödinger equation (TDSE) within the framework of the time-dependent Fourier grid Hamiltonian method (TDFGH). The numerical study has been backed up by a low order perturbative analysis wherever feasible. The plan of the paper is as follows. In § 2 we invoke the first order time-dependent perturbation theory to obtain the qualitative features of the bound state population dynamics for short-time scales. The time-dependent Fourier grid Hamiltonian method [11–12] is employed for obtaining more accurate and quantitative information on the bound state population as well as dissociation dynamics (§ 3). The main features of the perturbative and numerical results are analyzed in § 4 for both continuous and pulsed irradiation.

2. Perturbative bound state dynamics

Since the diatomic molecule is represented by a Morse potential, the unperturbed Hamiltonian (H_0) is given by

$$H_0 = \frac{p^2}{2m} + D_{AB}^0 \{1 - \exp[-\beta(x - x_{\text{eq}})]\}^2. \quad (1)$$

The parameters of H_0 are so chosen as to describe the bound vibrational levels of hydrogen molecule [$D_0 = 0.17440$ a.u., $\beta = 1.02764$ a.u., $x_{\text{eq}} = 1.40201$ a.u.].

Now let us suppose that the well-depth D_{AB}^t of the oscillator oscillates with time. If the time-dependent well-depth be represented by D_{AB}^t , the Hamiltonian becomes time-dependent.

$$H_t = \frac{p^2}{2m} + D_{AB}^t \{1 - \exp[-\beta(x - x_{\text{eq}})]\}^2 \quad (2)$$

where we have chosen $D_{AB}^t = D_{AB}^0 + \Delta D f(t)$, $f(t)$ being the temporal modulator of ΔD such that at $t = 0$, $H_t = H_0$. A simple choice for $f(t)$ is $f(t) = \sin \omega t$. As time proceeds, the well-depth D_{AB}^t therefore varies sinusoidally. The Hamiltonian H_t is manifestly phenomenological. But we may offer some rationalization in the following way. If the Morse oscillator (H_0) interacts weakly with the surrounding (H_s) through an interaction term V_{0s} , the equilibrated system eigenstates can be found by solving the following eigenvalue equation [20].

$$\begin{pmatrix} H_0 & V_{s0} \\ V_{s0}^+ & H_s \end{pmatrix} \begin{pmatrix} C_0 \\ C_s \end{pmatrix} = E \begin{pmatrix} C_0 \\ C_s \end{pmatrix}. \quad (2a)$$

Morse oscillator

Equation (2a) can be split into a pair of coupled eqs (2b) and (2c)

$$H_0 C_0 + V_{0s} C_s = EC_0 \quad (2b)$$

$$V_{s0}^+ C_0 + H_s C_s = EC_s. \quad (2c)$$

Using the fact that $C_s = -(H_s - E)^{-1} V_{s0}^+ C_0$, we can recast (2a) as

$$[H_0 - V_{0s}(H_s - E)^{-1} V_{s0}^+] C_0 = EC_0$$

which can be written as

$$[H_0 + V_{\text{eff}}] C_0 = EC_0$$

i.e.,

$$H_{\text{eff}} C_0 = EC_0.$$

Over a long-time scale V_{eff} may be replaced by a time-averaged interaction and be treated as a constant quantity. But while probing on a very short-time scale one would notice a time-varying V_{eff} . We have treated V_{eff} as a sinusoidally oscillating term so that $H_{\text{eff}} \rightarrow H_0$ as $t \rightarrow 0$ and V_{eff} averaged over a characteristic period of oscillation is zero. This simplifies the problem greatly.

The other perturbation present in the system is external and works on a faster time scale. The characteristics of the time-varying field which couples with the oscillator are as follows,

$$V'(x, t) = \varepsilon_0 S(t) x \sin \omega t;$$

where ε_0 is the electric field strength and ω the laser frequency, and $S(t)$ is a pulse shape function. When the field is continuous, $S(t) = 1$. For pulsed fields $S(t)$ can have many different forms. However, we shall make use of the following three forms only in the present study:

$$(i) S(t) = \sin^2 \frac{\pi t}{t_p};$$

$$(ii) S(t) = 1 - \left| 1 - \frac{2t}{t_p} \right|;$$

$$(iii) S(t) = \exp[-\gamma(t - t_p)^2]$$

where t_p stands for the pulse duration. So the total Hamiltonian representing a Morse oscillator with oscillating well-depth and interacting with an external time-varying field is given by

$$H(t) = \frac{p^2}{2m} + \left[D_{AB}^0 + \Delta D \sin \frac{2\pi t}{\tau} \right] (1 - \exp[-\beta(x - x_{\text{eq}})])^2 + \varepsilon_0 S(t) x \sin \omega t \quad (3)$$

$$\begin{aligned} &= \frac{p^2}{2m} - D_{AB}^0 (1 - \exp[-\beta(x - x_{\text{eq}})])^2 + \Delta D \sin \frac{2\pi t}{\tau} \\ &\quad \times (1 - \exp[-\beta(x - x_{\text{eq}})])^2 + \varepsilon_0 S(t) x \sin \omega t \\ &= H_0 + H_1(t) + H_2(t) \end{aligned} \quad (4)$$

where

$$H_1 = \Delta D \sin \frac{2\pi t}{\tau} (1 - \exp[-\beta(x - x_{eq})])^2 \quad \text{and} \quad H_2 = \varepsilon_0 S(t) x \sin \omega t.$$

The zeroth order Hamiltonian (H_0) is clearly the free Morse oscillator Hamiltonian of constant well-depth D_{AB}^0 .

Now we consider the different cases that may arise; for e.g. (i) when the external time-varying field is present but the well-depth does not oscillate, i.e., $\varepsilon_0 \neq 0$, but $\Delta D = 0$; (ii) when the well-depth oscillates but the field is absent, i.e., $\varepsilon_0 = 0$, but $\Delta D \neq 0$; (iii) when the well-depth oscillates and the applied field intensity is non-zero, i.e., $\varepsilon_0 \neq 0$ and $\Delta D \neq 0$. In what follows we make a perturbative estimate of the population of different levels, assuming a short-time interval and not too high fields.

(i) when $\varepsilon_0 \neq 0$, but $\Delta D = 0$:

If $\varepsilon_0 \neq 0$ and $\Delta D = 0$, the Hamiltonian of the system becomes

$$H(t) = H_0 + H_2(t)$$

where

$$H_2(t) = \varepsilon_0 S(t) x \sin \omega t. \quad (5)$$

For the sake of simplicity we consider that the field is continuous i.e. $S(t) = 1$. Thus,

$$H_2(t) = \varepsilon_0 x \sin \omega t.$$

Let the system be in the m th eigenstate of H_0 , (Φ_m^0) at $t = 0$. The perturbation throws Φ_m^0 into a linearly superposed state $\Psi(t)$ with

$$\Psi(t) = \sum_{k=1}^N a_k(t) \Phi_k^0 \exp(-iE_k^0 t/\hbar);$$

where

$$H_0 \Phi_k^0 = E_k^0 \Phi_k^0 \quad \text{and}$$

$$i\hbar \frac{\delta \Psi}{\delta t} = (H_0 + H_2(t)) \psi.$$

In the first order therefore the transition probability from an initial eigenstate (n) of the unperturbed Morse oscillator (H_0) to a state (m) caused by the applied field is given by

$$\begin{aligned} |a_m^1(t, \varepsilon_0)|^2 &= \frac{\varepsilon_0^2 \langle m|x|n \rangle^2}{4\hbar^2} \left[\frac{4 \sin^2(\omega_{mn} - \omega)t/2}{(\omega_{mn} - \omega)^2} - \frac{1}{(\omega_{mn}^2 - \omega^2)} \right. \\ &\quad \times \left[2 \sin(\omega + \omega_{mn})t/2 \sin(\omega_{mn} - \omega)t/2 + 4 \sin^2(\omega_{mn} - \omega)t/2 \right] \\ &\quad \left. + \frac{4 \sin^2(\omega_{mn} + \omega)t/2}{(\omega_{mn} + \omega)^2} \right] = P_{mn}^1(t, \varepsilon) \end{aligned}$$

where

$$a_m^1(t, \varepsilon_0) = \frac{\varepsilon_0 \langle m|x|n \rangle}{2i\hbar} \left[\frac{\exp i(\omega_{mn} - \omega)t - 1}{(\omega_{mn} - \omega)} - \frac{\exp i(\omega_{mn} + \omega)t + 1}{(\omega_{mn} + \omega)} \right] \quad (6)$$

Morse oscillator

and $\langle m|x|n\rangle = \langle \Phi_m^0|x|\Phi_n^0\rangle$, $\omega_{mn} = (E_m^0 - E_n^0)/\hbar$; and ε_0 is the electric field strength of the applied radiation, ω is its frequency which is supposed to be slightly off-resonance. $|a_m^1(t, \varepsilon)|^2$ or $P_{mm}^1(t, \varepsilon)$ is then the population of the m th state of the unperturbed Morse oscillator created by the applied off-resonance time-varying electric field of the radiation.

(ii) when $\varepsilon_0 = 0$ but $\Delta D \neq 0$

In this case,

$$H(t) = H_0 + H_1(t)$$

where

$$H_1(t) = \Delta D \sin(2\pi t/\tau) [(1 - \exp[-\beta(x - x_{\text{eq}})])^2].$$

Now expanding the exponential term and considering only terms up to $(x - x_{\text{eq}})^2$ we obtain,

$$H_1(t) = H_1^{(1)}(t) = \Delta D \sin(2\pi t/\tau) \beta (x - x_{\text{eq}})^2.$$

The first order transition amplitude $a_m^1(t)$ is therefore given by

$$a_m^1(t, \Delta D) = \frac{\Delta D \beta^2}{4i\hbar} \langle m|(x - x_{\text{eq}})^2|n\rangle \times \left[\frac{\exp i(\omega_{mn} - (2\pi/\tau))t - 1}{(\omega_{mn} - (2\pi/\tau))} - \frac{\exp i(\omega_{mn} + (2\pi/\tau))t - 1}{(\omega_{mn} + (2\pi/\tau))} \right].$$

The first order transition probability from the state n to the state m due to oscillations of the well-depth alone is therefore given by

$$|a_m^1(t, \Delta D)|^2 = P_{mm}^1(t, \Delta D) = \frac{(\Delta D)^2 \beta^4}{16 \hbar^2} \langle m|(x - x_{\text{eq}})^2|n\rangle^2 \times \left[\frac{4 \sin^2(\omega_{mn} - (2\pi/\tau))t/2}{(\omega_{mn} - (2\pi/\tau))^2} - \frac{1}{(\omega_{mn} - (4\pi^2/\tau))} \right] \times \left(4 \sin\left(\omega_{mn} + \frac{2\pi}{\tau}\right)t/2 - \sin\left(\omega_{mn} - \frac{6\pi}{\tau}\right)t/2 + 4 \sin^2\left(\omega_{mn} + \frac{2\pi}{\tau}\right)t/2 + 4 \frac{\sin^2(\omega_{mn} + (2\pi/\tau))t}{(\omega_{mn} + (2\pi/\tau))^2} \right) \quad (7)$$

$P_{mm}^{(1)}(t, \Delta D)$ in fact gives the population of the m th vibrational level of the unperturbed Morse oscillator of well-depth D_0^{AB} created by a sinusoidal temporal fluctuation of the well-depth with an amplitude ΔD .

(iii) when both $\varepsilon_0 \neq 0$ and $\Delta D \neq 0$

In this case

$$H(t) = H_0 + H_1(t) + H_2(t) = H_0 + H'(t)$$

$$H'(t) = \Delta D \sin(2\pi t/\tau) [1 - \exp[-\beta(x - x_{\text{eq}})]]^2 + \varepsilon_0 x \sin \omega t.$$

Now making approximations already introduced in (ii), we may write $H'(t)$ as

$$H'(t) = H^{(1)}(t)\Delta D \sin(2\pi t/\tau)\beta(x - x_{eq}^2)^2 + \varepsilon x \sin \omega t.$$

The first order transition amplitude for the oscillator with oscillating well-depth in the presence of the applied time-varying non-resonant field is then given by

$$a_m^1(t, \varepsilon_0 \Delta D) = \frac{\varepsilon_0 \langle n|x|n \rangle}{2i\hbar} \left[\frac{\exp i(\omega_{mn} - \omega)t - 1}{(\omega_{mn} - \omega)} - \frac{\exp i(\omega_{mn} + \omega)t + 1}{(\omega_{mn} + \omega)} \right] \\ + \frac{\Delta D \beta^2}{4i\hbar} \langle m|(x - x_{eq})^2|n \rangle \left[\frac{\exp i(\omega_{mn} - (2\pi/\tau))t - 1}{(\omega_{mn} - (2\pi/\tau))} \right. \\ \left. - \frac{\exp i(\omega_{mn} + (2\pi/\tau))t - 1}{(\omega_{mn} + (2\pi/\tau))} \right].$$

The corresponding transition probability from an initial unperturbed state n to the final perturbed state m caused by the oscillating well-depth and time-varying electric field of the radiation that act in unison is therefore given by

$$|a_m^1(t, \varepsilon_0, \Delta D)|^2 = P_{mn}^1(t, \varepsilon_0, \Delta D) = \\ \frac{\varepsilon_0^2 \langle m|x|n \rangle^2}{4\hbar^2} \left[\frac{4 \sin^2(\omega_{mn} - \omega)t/2}{(\omega_{mn} - \omega)^2} - \frac{1}{(\omega_{mn}^2 - \omega^2)} \left[2 \sin(\omega + \omega_{mn})t/2 \right. \right. \\ \left. \left. \times \sin(\omega_{mn} - \omega)t/2 + 4 \sin^2(\omega_{mn} - \omega)t/2 \right] + \frac{4 \sin^2(\omega_{mn} + \omega)t/2}{(\omega_{mn} + \omega)^2} \right] \\ + \frac{(\Delta D)^2 \beta^4}{16\hbar^2} |\langle m|(x - x_{eq})^2|n \rangle|^2 \left[\frac{4 \sin^2(\omega_{mn} - (2\pi/\tau))t/2}{(\omega_{mn} - (2\pi/\tau))^2} - \frac{1}{(\omega_{mn} - (4\pi^2/\tau))} \right. \\ \left. \times \left(4 \sin\left(\omega_{mn} + \frac{2\pi}{\tau}\right)t/2 - \sin\left(\omega_{mn} - \frac{6\pi}{\tau}\right)t/2 + 4 \sin^2\left(\omega_{mn} + \frac{2\pi}{\tau}\right)t/2 \right) \right. \\ \left. + \frac{4 \sin^2(\omega_{mn} + (2\pi/\tau))t}{(\omega_{mn} + (2\pi/\tau))^2} \right] + \frac{\Delta D \beta^2 \varepsilon_0 \langle (x - x_{eq})^2 \rangle_{mn}}{8\hbar^2} \\ + \left[\frac{2 \cos(\omega - (2\pi/\tau))t - 2 \cos(\omega_{mn} - (2\pi/\tau))t - 2 \cos(\omega_{mn} - \omega)t + 2}{(\omega_{mn} - (2\pi/\tau))(\omega_{mn} - \omega)} \right. \\ \left. - \frac{2 \cos(\omega + (2\pi/\tau))t - 2 \cos(\omega_{mn} - (2\pi/\tau))t - 2 \cos(\omega_{mn} + \omega)t + 2}{(\omega_{mn} - (2\pi/\tau))(\omega_{mn} + \omega)} \right. \\ \left. - \frac{2 \cos(\omega + (2\pi/\tau))t - 2 \cos(\omega_{mn} + (2\pi/\tau))t - 2 \cos(\omega_{mn} - \omega)t + 2}{(\omega_{mn} + (2\pi/\tau))(\omega_{mn} - \omega)} \right. \\ \left. + \frac{2 \cos(\omega - (2\pi/\tau))t - 2 \cos(\omega_{mn} + (2\pi/\tau))t - 2 \cos(\omega_{mn} + \omega)t + 2}{(\omega_{mn} + (2\pi/\tau))(\omega_{mn} + \omega)} \right] \\ = P'_{mn}(t, \varepsilon, \Delta D = 0) + P'_{mn}(t, \varepsilon = 0, \Delta D) + P'_{mn}(t, \varepsilon_0, \Delta D) \quad (8)$$

Morse oscillator

$P'_{mm}(t, \varepsilon_0, \Delta D)$ represents the part of the time-dependent population of the m th state of the unperturbed Morse oscillator (H_0) that is created by the interference of the population excitation–deexcitation dynamics caused by well-depth oscillation and the applied time-varying field. The overall expression of $P'_{mm}(t, \varepsilon_0, \Delta D)$ suggests a parabolic dependence of the population on the electric field strength (ε_0) when all other system parameters viz., ΔD , β , etc., are fixed. The expression also reveals parabolic dependence of P'_{mm} on ΔD at fixed ε_0 and β . However, these are first order results and are therefore of limited validity. We therefore propose to calibrate these predictions against near exact solutions of the corresponding TDSE equation by invoking the TDFGH method proposed earlier by Adhikari *et al* [11–12] and later extensively applied by Sarkar *et al* [21–22]. Since the TDFGH method is not yet widely known, we would briefly discuss the salient features of the method.

TDFGH method

Let us start with the TDSE,

$$i\hbar \frac{\delta\Psi}{\delta t} = H\Psi \quad (9)$$

where

$$H = H_0 + V'(x, t) = \frac{p^2}{2m} + V(x) + V'(x, t). \quad (10)$$

We can employ the FGH method [23–24] to evaluate the eigenfunctions and eigenvalues of H_0 giving

$$H_0|\Phi_i^0(x)\rangle = \varepsilon_i^0|\Phi_i^0(x)\rangle, \quad i = 1, 2, \dots, N, \quad (11)$$

where N is the number of grid points used for representing $|\Phi_i^0\rangle$ in the co-ordinate space.

$$|\Phi_i^0\rangle = \sum_{i=1}^N |x_i\rangle \Delta x w_i^0 \quad (12)$$

$\{w_i^0\}$ in (12) represent the values of the co-ordinate representative of the state function $|\Phi_i^0(x)\rangle$ at the grid points, the values of which are obtained by the standard variational recipe [23–24]. The FGH method can be used to propagate the wave function on the same grid as shown by Adhikari *et al* [11–12]. Thus, when the perturbation is switched on, the state function $\Psi(x, t)$ is given by

$$|\Psi(x, t)\rangle = \sum_{i=1}^N |x_i\rangle \Delta x w_i(t). \quad (13)$$

The amplitudes ($w_i(t)$) are now time-dependent quantities and their evolution equations are as follows

$$w_j = \frac{1}{i\hbar} \sum_i [\langle x_j | H_0 | x_i \rangle + \langle x_j | V(x, t) | x_i \rangle] w_i(t). \quad (14)$$

Once initial values of $\{w_i\}$ are specified, (14) can be numerically integrated on the specified grid by Runge–Kutta or Bulirsch–Stoer method [25]. The matrix elements of

H_0 and V of (14) can be evaluated using the FGH method

$$\langle x_i | H_0 | x_j \rangle = \frac{1}{\Delta x} \left[\sum_{l=-n}^n \frac{\exp[2\pi l(i-j)/n]}{N} \right] \{ T_1 \} + V(x_i, t) \delta_{ij} \quad (15)$$

where

$$T_1 = [\hbar^2/2m](l\Delta k)^2, \quad \Delta k = (2\pi/N\Delta x) \quad \text{and} \quad 2n = N - 1$$

and

$$\langle x_i | V(x, t) | x_j \rangle = V(x_i, t) \delta(x_i - x_j) \quad (16)$$

Once $w_i(t)$ and hence $\Psi(x, t)$ are obtained, the projections of $\Psi(x, t)$ onto the eigenstates of H_0 generate time-dependent overlap amplitudes

$$S_i(t) = |\langle \Phi_i^0 | \Psi(x, t) \rangle|^2, \quad i = 1, 2, 3, \dots, N. \quad (17)$$

The $S_i(t)$ essentially represent the population of the i th eigenstate of the unperturbed Hamiltonian at a time $\{t\}$ after the perturbation is switched on. If the system is initially in the unperturbed ground state, $S_1(0) = 1$ and $S_j(0) = 0$ ($j \neq 1$). For $t > 0$, $S_i(t)$ begin to change with time as the perturbation V causes excitations to occur with respect to the unperturbed system. $S_i(t)$ s, therefore, provide a complete description of the dynamics of level population in terms of which changes in all observables can be calculated and interpreted. Once the oscillator is excited to an unbound level, dissociation takes place. Using the $S_i(t)$ values, we can therefore define the dissociation probability P_d as follows,

$$P_d(t) = 1 - \sum_i^{n_b} \langle |\Psi(x, t) | \Phi_i^0 \rangle|^2 = 1 - \sum_i S_i(t). \quad (18)$$

In (18), n_b stands for the number of bound states supported by the unperturbed Hamiltonian (i.e. the free Morse oscillator of constant well-depth, in this case). In what follows, we discuss the numerical results obtained from TDFGH method and the expectations based on first order perturbation theory.

3. Results and discussion

(i) Bound state population dynamics

Figure 1(a) shows the growth and decay of the population of the ground and the first three excited vibrational levels of the Morse oscillator with constant well-depth ($\Delta D = 0$) computed numerically by the TDFGH recipe, as the electric field of the applied radiation interacts with it. Figure 1(b) shows the perturbatively computed population [eq. (6)] versus time profile of the first excited state. The population versus time profiles for other excited states have more or less identical features. The similarity of the nature of the population dynamics of the excited states calculated numerically and perturbatively establishes the validity of the first order TDPT over the time-scale of our analysis and for the strengths of the perturbations used. Figure 2 shows the numerically calculated population versus time profiles of the ground and the first three excited states of the Morse oscillator in the presence of radiation when the well-depth oscillates sinusoidally with time. The main features of the bound level population dynamics are identical with those observed for the constant well-depth case. The conclusion is therefore that the oscillating well-depth does not alter the gross dynamical

Morse oscillator

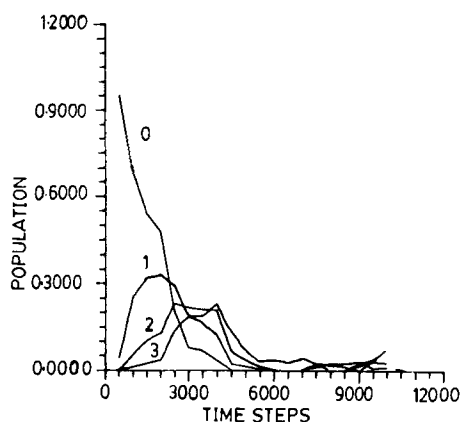


Figure 1(a). Growth and decay of level populations of the ground and the first three excited states of a Morse oscillator with constant well-depth as the electric field of the applied radiation interacts with it.

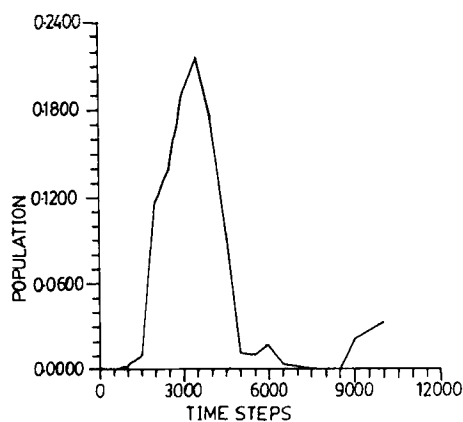


Figure 1(b). Perturbatively computed population versus time profile of the first excited state of the same system depicted in figure 1(a).

features of the population-time profiles, although the excitation or relaxation rates in the presence of the well-depth oscillation may be quite different from their constant well-depth counterparts (see later).

Figure 3(a) shows the numerically computed (by TDFGH method) population of a vibrational level ($k = 2$) of the Morse oscillator with oscillating well-depth ($\Delta D \neq 0$) as a function of the intensity (ϵ_0) of the applied field. The overall parabolic nature of the profile mirrors the prediction of the first order TDPT. Figure 3(b) shows the behaviour of the numerically computed population $P_{kk}(t) - \Delta D$ profile for a fixed value of ' ϵ_0 ', the applied field strength. From the figure it is seen that the population of the given state monotonically increases as ΔD increases. Thus, the perturbation theoretical prediction that the dependence of the population on ΔD would be parabolic for a fixed value of ϵ_0

is not echoed by the numerical results. May be, much smaller ΔD values would have ensured the validity of the particular perturbative result. Figure 3(c) shows the population dynamics of the three highest bound vibrational levels for the $\Delta D \neq 0$ case which is basically similar to that observed for the lower states. From the observed population dynamics it appears that if the applied field intensity is below a certain threshold, excitation is the only process to reckon with and the dissociation probability is negligible. Once the threshold is crossed, rapid onset of dissociation of the diatomic molecule sets in. It would therefore be interesting to know how the dissociation

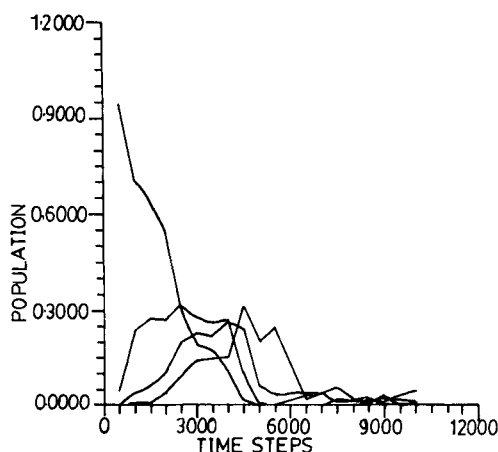


Figure 2. Growth and decay of level populations of the ground and the first three excited states of the Morse oscillator in the presence of the radiation when well-depth oscillates sinusoidally with time.

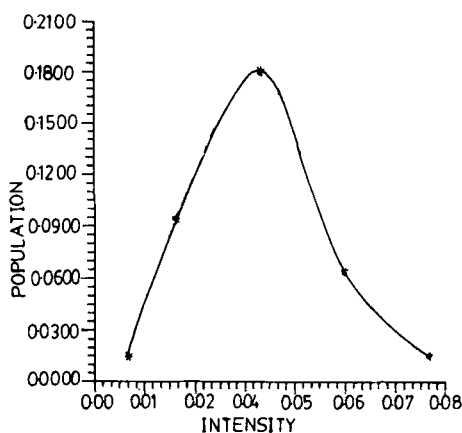


Figure 3(a). Numerically computed population (by the TDFGH method) of a vibrational level ($k = 2$) of a Morse oscillator with oscillating well-depth ($\Delta D \neq 0$) as a function of the intensity (ϵ) of the applied field.

Morse oscillator

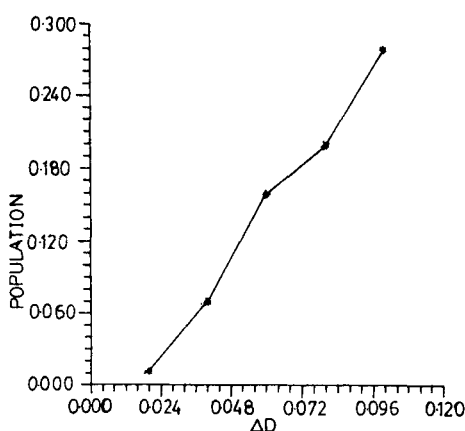


Figure 3(b). Numerically computed population of the $k=2$ level shown as a function of ΔD for a fixed value of ε , the strength of the applied field.

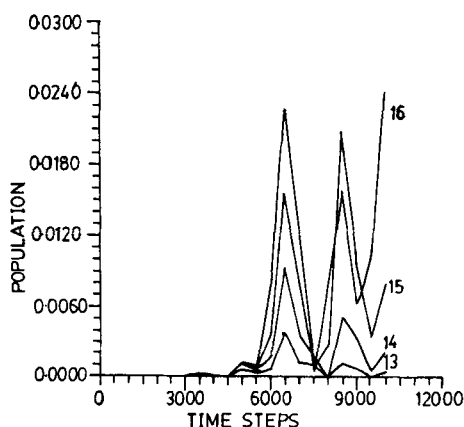


Figure 3(c). Numerically computed population versus time profiles of the three highest bound vibrational levels.

probability depends upon the applied field intensity, when the well-depth oscillates. The specific questions to be probed are the following. Does the well-depth oscillation alter the dissociation dynamics observed for a constant well-depth Morse oscillator? Is there any pulse-shape effect on the temporal characteristics of the dissociation process? Before focussing on these aspects of the problem, we would like to see whether an oscillating well-depth affects the excitation or relaxation rates induced by the field.

Let us suppose that we start with the system in the ground state of the unperturbed oscillator at $t = 0$. Figures 3(d) and (e) show the growth of the population of the first excited state as the applied field interacts with the Morse oscillator of (i) fixed, and (ii) oscillating well-depth, respectively. The limiting slopes of these curves give the total

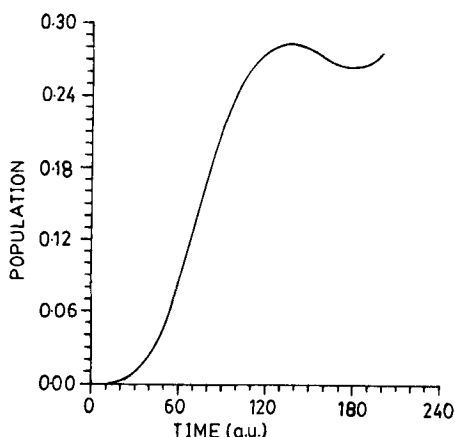


Figure 3(d). Growth of the population of the first excited state as the applied field interacts with the Morse oscillator of fixed well-depth ($\varepsilon = 0.06$, $\Delta D = 0.0$).

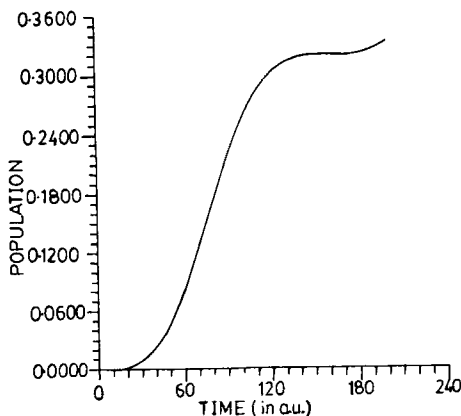


Figure 3(e). Growth of the population of the first excited state as the applied field interacts with the Morse oscillator of oscillating well-depth ($\varepsilon = 0.06$, $\Delta D = 0.087$).

rate of excitation into the first excited state, which are recorded in table 1. For a Morse oscillator with a time-dependent well-depth, the excitation rate is larger showing constructive interference between the field-induced and the oscillating well-depth controlled excitations. If we start with the oscillator in an excited state, we can similarly compute the rate of relaxation caused by the external field as well as by the internal perturbation set up in the system due to oscillation in the well-depth. For $k = 1$ level, these rates are also reported in table 1 both when $\Delta D = 0$, $\varepsilon_0 \neq 0$ and $\Delta D \neq 0$, $\varepsilon_0 \neq 0$. Thus, the well-depth oscillation is seen to enhance the excitation rates but depress the relaxation rates in a Morse oscillator interacting with the radiation.

Table 1. Computed excitation and relaxation rates of a given vibrational level of a Morse oscillator in the absence and presence of well-depth oscillation.

System	Rate of excitation to the first excited state (ps^{-1})	Rate of relaxation of the first excited state (ps^{-1})
i) Morse oscillator with fixed well-depth	i) 1.79	i) 8.30
ii) Morse oscillator with oscillating well-depth	ii) 2.84	ii) 6.16

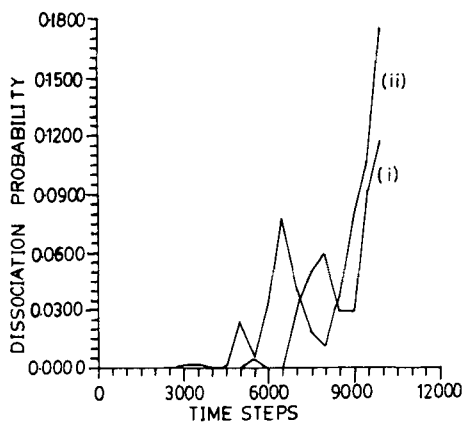


Figure 4(a). Dissociation probability versus time profile for the oscillator with (i) fixed well-depth (ii) oscillating well-depth, for a fixed value of ϵ_0 .

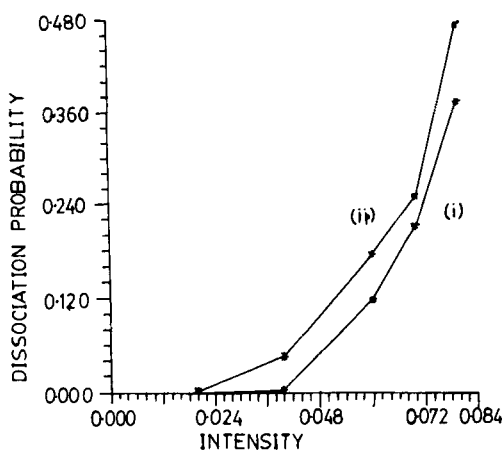


Figure 4(b). Computed dissociation probability P_d as a function of the intensity of the applied field of the laser for the oscillator with (i) time-invariant well-depth (ii) time-varying well-depth.

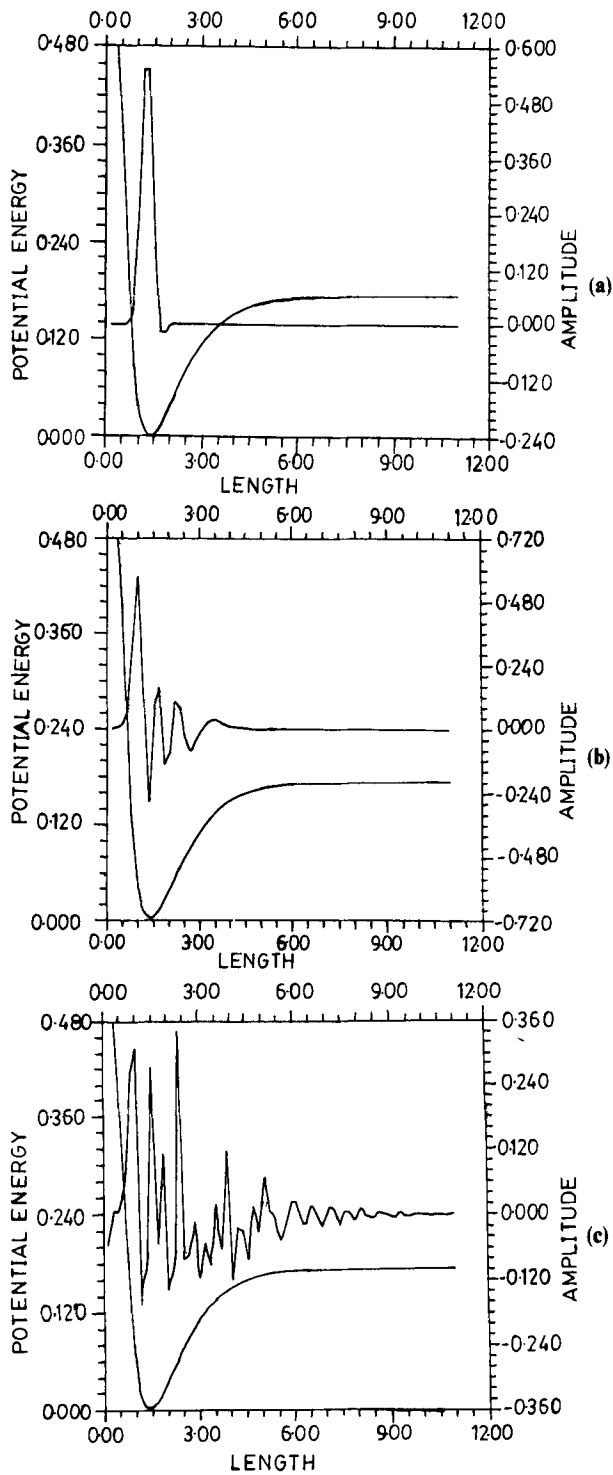


Figure 5(a-c). Profiles of the ground state vibrational wave function of H_2 (modelled by a morse oscillator) as it dissociates under laser irradiation. (a) $\Psi(x, t)$ at $t = 0$; (b) $\Psi(x, t)$ at $t = 10$ fs (c) $\Psi(x, t)$ at $t = 25$ fs. The peak intensity of the pulse is $\epsilon_0 = 0.06$ a.u.

(ii) Dissociation dynamics

(a) *Dissociation probability, time and intensity thresholds:* We first consider the case, when the field is continuous. Figure 4(a) shows the P_d -time profile for the oscillator (i) with fixed well-depth (ii) with oscillating well-depth, for a fixed value of ε_0 . The oscillating well-depth is seen to lower the time-threshold slightly with respect to the constant well-depth Morse oscillator.

Figure 4(b) shows how the computed dissociation probability of a Morse oscillator at a given time (t) varies with the intensity of the applied time-varying field with (i) time-invariant well-depth, (ii) time-varying well-depth. In both cases, a clear threshold intensity ($\varepsilon^0 = \varepsilon_0$) is seen to exist beyond which the dissociation probability rises sharply. From the figures, one would be tempted to conclude that, the oscillation of well-depth lowers the threshold intensity compared to that observed in the constant well-depth case, when illumination is continuous.

We have monitored at this point the wave function as the molecule dissociates. Figures 5(a–c) show the wavefunction at different stages of evolution after the field is switched on. As the system gains energy from perturbing field, more and more nodes appear in $\Psi(x, t)$ and the effective spatial extension of $\Psi(x, t)$ increases.

When a pulsed field is used, the picture that emerges from the continuous-field-oscillator model is seen to change a lot. Figure 6(a) shows how the dissociation probability varies with the field intensity ε_0 in (i) the fixed well-depth case, (ii) the oscillating well-depth case, when the intensity varies as $\sin^2(\pi t/t_p)$. From the figures a picture opposite to that observed in the continuous field case is seen to emerge i.e., the oscillating well-depth increases the threshold intensity of dissociation when a pulsed field is used. Figure 6(b) shows the dissociation probability versus time profile in (i) continuous laser field; (ii) pulsed laser field with \sin^2 dependence; (iii) triangularly pulsed laser field; (iv) laser with Gaussian pulse shape, when the peak intensity (ε_0) and laser frequency (ω) are the same in each case. From the figures it is seen that compared

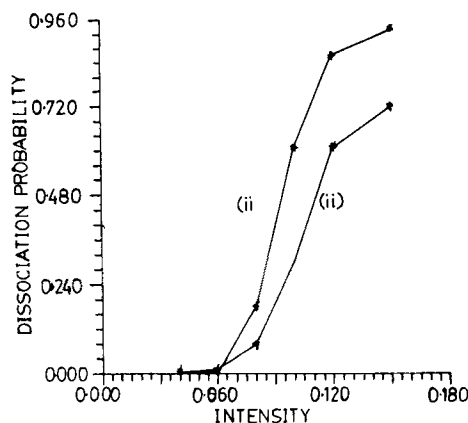


Figure 6(a). Dissociation probability versus intensity profile for the oscillator with (i) fixed well-depth (ii) oscillating well-depth for pulsed laser fields.

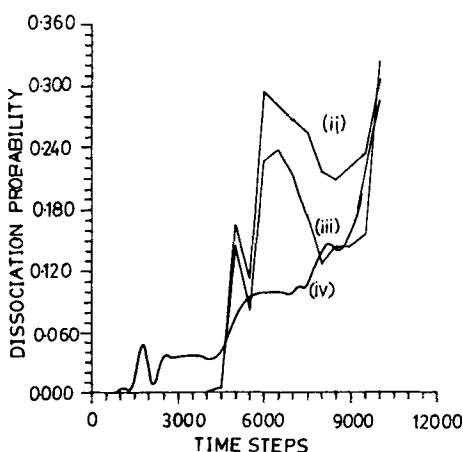
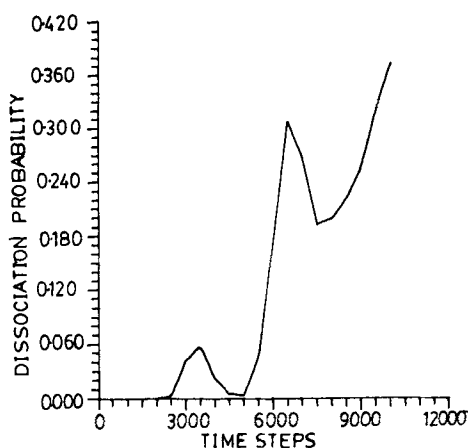


Figure 6(b). Dissociation probability versus time profile for (i) continuous laser field (ii) pulsed laser field with \sin^2 dependence (iii) triangularly pulsed laser field. (iv) Gaussian pulsed laser field.

to continuous irradiation, the pulsed laser field lowers the dissociation probability of the diatom at any given time. But the gross features of the P_d versus time profile for three different types of pulsed fields are not very different [4–5]. It would be interesting to analyze the kind of effects that a Morse oscillator with a randomly oscillating well-depth would bring about. We will address ourselves to this problem in a future communication.

4. Conclusions

By studying the bound state population and dissociation dynamics of a model diatomic species whose binding energy oscillates with time, we come to the following conclusions:

- (i) The bound state population dynamics as predicted by first order TDPT, *almost* corroborates with the numerical results obtained from near exact TDFGH calculations as long as the perturbation is small and short-time scales are considered.
- (ii) When the well-depth oscillates slowly, which is the actual situation when the system interacts with the surrounding medium, the threshold intensity decreases to a small extent for dissociation under continuous irradiation; but, for pulsed fields, oscillating well-depth is predicted to increase the threshold intensity of dissociation.
- (iii) The nature of the dissociation probability versus time profiles and the actual extent of dissociation appears to be almost the same for pulses of different shapes that we have studied. However, a different choice of V_{eff} could change the picture completely. The problems of microscopic derivation of V_{eff} and thus, H_{eff} and a fully quantum dynamical study of the processes of our interest are presently under way.

Acknowledgement

One of us (PS) wishes to thank the Council of Scientific and Industrial Research, Government of India, New Delhi, for the award of a Junior Research Fellowship.

References

- [1] A D Bandrauk, ed., *Atomic and molecular processes with short intense laser pulses* (Plenum, New York, 1988)
- [2] M Quack, In *Advances in chemical physics*, (Wiley, New York, 1982) Vol 50
- [3] H P Breuer, K Dietz and M Holthaus, *Z. Phys.* **D8**, 349 (1988); **D11**, 1 (1989)
- [4] S Chelkowski and A D Bandrauk, *Phys. Rev.* **A41**, 6480 (1990)
- [5] S Chelkowski, A D Bandrauk and P B Corkum, *Phys. Rev. Lett.* **65**, 2355 (1990)
- [6] M E Goggin and P W Milonni, *Phys. Rev.* **A37**, 796 (1988)
- [7] V S Letokhov, In *Non-linear laser chemistry* (Springer, Berlin, 1988) ch. 5
- [8] N Bloembergen and A H Zewail, *J. Phys. Chem.* **88**, 5459 (1984)
- [9] R C Brown and R E Wyatt, *J. Phys. Chem.* **90**, 3590 (1986); *Phys. Rev. Lett.* **57**, 1 (1986)
- [10] G Gangopadhyay and D S Ray, *J. Chem. Phys.* **97**, 4104 (1992)
- [11] S Adhikari, P Dutta and S P Bhattacharyya, *Chem. Phys. Lett.* **199**, 574 (1992); *Int. J. Quantum Chem.* (to appear, 1995)
- [12] S Adhikari and S P Bhattacharyya, *Phys. Lett.* **A172**, 155 (1992); *Proc. Indian Acad. Sci. (Chem. Sci.)* (1994)
- [13] J Javanawnen, J H Eberly and Q Su, *Phys. Rev.* **A38**, 3430 (1988)
- [14] J N Bardsley, A Szoke and M J Comella, *J. Phys.* **B21**, 3430 (1988)
- [15] J N Bardsley and M J Comella, *Phys. Rev.* **A39**, 2252 (1989)
- [16] B Just, J Nanz and G K Paramonov, *Chem. Phys. Lett.* **193**, 429 (1992)
- [17] B Just, J Nanz and I Trisca, *Chem. Phys. Lett.* **193**, 423 (1992)
- [18] G K Paramonov, *Chem. Phys. Lett.* **169**, 573 (1990)
- [19] M Quack and E Sutcliffe, *Infrared Phys.* **25**, 163 (1985)
- [20] R McWeeny, *Methods of molecular quantum mechanics* 2nd ed. (1989) A.P. (N.Y.)
- [21] P Sarkar, S Adhikari and S P Bhattacharyya, *Chem. Phys. Lett.* **227**, 187 (1994)
- [22] P Sarkar and S P Bhattacharyya, *Int. J. Quantum Chem.* 1995 (in press)
- [23] C C Marston and G G Balint Kurti, *J. Chem. Phys.* **91**, 3571 (1989)
- [24] G G Balint Kurti, C L Ward and C C Marston, *Comput. Phys. Commun.* **67**, 285 (1991)
- [25] J Stoer and R Bulirsch, *Introduction to numerical analysis* (New York, Springer, 1980) sec. 7.2.14